UNLV | UNIVERSITY LIBRARIES

Mechanical Engineering Faculty Publications | Mechanical Engineering

2011

Streaming Potential Generated by a Pressure-Driven Flow Over Superhydrophobic Stripes

Hui Zhao
University of Nevada, Las Vegas, hui.zhao@unlv.edu

Follow this and additional works at: https://digitalscholarship.unlv.edu/me_fac_articles

Part of the Acoustics, Dynamics, and Controls Commons, Nanoscience and Nanotechnology Commons, and the Power and Energy Commons

Repository Citation

Zhao, H. (2011). Streaming Potential Generated by a Pressure-Driven Flow Over Superhydrophobic Stripes. *Physics of Fluids, 23*(2), 022003-1-022003-10.
https://digitalscholarship.unlv.edu/me_fac_articles/556

This Article is protected by copyright and/or related rights. It has been brought to you by Digital Scholarship@UNLV with permission from the rights-holder(s). You are free to use this Article in any way that is permitted by the copyright and related rights legislation that applies to your use. For other uses you need to obtain permission from the rights-holder(s) directly, unless additional rights are indicated by a Creative Commons license in the record and/or on the work itself.

This Article has been accepted for inclusion in Mechanical Engineering Faculty Publications by an authorized administrator of Digital Scholarship@UNLV. For more information, please contact digitalscholarship@unlv.edu.

AIP | Physics of Fluids

Streaming potential generated by a pressure-driven flow over superhydrophobic stripes

Hui Zhao

Citation: Phys. Fluids **23**, 022003 (2011); doi: 10.1063/1.3551616
View online: http://dx.doi.org/10.1063/1.3551616
View Table of Contents: http://pof.aip.org/resource/1/PHFLE6/v23/i2
Published by the AIP Publishing LLC.

Additional information on Phys. Fluids

Journal Homepage: http://pof.aip.org/
Journal Information: http://pof.aip.org/about/about_the_journal
Top downloads: http://pof.aip.org/features/most_downloaded
Information for Authors: http://pof.aip.org/authors

ADVERTISEMENT

Downloaded 13 Aug 2013 to 131.216.164.149. This article is copyrighted as indicated in the abstract. Reuse of AIP content is subject to the terms at: http://pof.aip.org/about/rights_and_permissions

Streaming potential generated by a pressure-driven flow over superhydrophobic stripes

Hui Zhao[a)]
Department of Mechanical Engineering, University of Nevada, Las Vegas, Nevada 89154, USA

(Received 6 September 2010; accepted 13 January 2011; published online 1 February 2011)

The streaming potential generated by a pressure-driven flow over a weakly charged slip-stick surface [the zeta potential of the surface is smaller than the thermal potential (25 mV)] with an arbitrary double layer thickness is theoretically studied by solving the Debye–Huckel equation and Stokes equation. A series solution of the streaming potential is derived. Approximate expressions for the streaming potential in the limits of thin double layers and thick double layers are also given in excellent agreement with the full solution. To understand the impact of the slip, the streaming potential is compared against that over a homogeneously charged smooth surface. Our results indicate that the streaming potential over a superhydrophobic surface can only be enhanced under certain conditions. Moreover, as the double layer thickness increases, the advantage of the superhydrophobic surface diminishes. In addition, the Onsager relation which directly relates the magnitude of electro-osmotic effect to that of the streaming current effect has been explicitly proved to be valid for thin and thick double layers and homogeneously charged superhydrophobic surfaces. Comparisons between the streaming current and electro-osmotic mobility for an arbitrary electric double layer thickness under various conditions indicate that the Onsager relation seems applicable for arbitrary weakly charged superhydrophobic surfaces although there is no general proof. Knowledge of the streaming potential over a slip-stick surface can provide guidance for designing novel and efficient microfluidic energy-conversion devices using superhydrophobic surfaces.
© *2011 American Institute of Physics*. [doi:10.1063/1.3551616]

I. INTRODUCTION

A pressure-driven flow drags excess counterions inside an electric double layer (EDL) to move near a charged surface, generating an electric current termed streaming current. In the absence of an external electrical load, a streaming potential is developed to balance the streaming current.[1] With the external electrical load, electric energy is harvested from the fluidic system.[2] This idea of converting hydrodynamics to electric power has received increasing interest with the development of microfluidic and nanofluidic devices which have an inherent advantage: high surface to volume ratio.[3–5] However, because only excess ions inside the EDL contribute to the streaming current and the no-slip boundary condition prevents the flow velocity from being substantial near the surface, current microfluidic and nanofluidic devices fall short of conversion efficiency and power density, limiting such a promising technology from being practically implemented.

To overcome the aforementioned limitations, hydrodynamic slip at a charged surface has been proposed to increase the efficiency by enhancing the electroconvection inside the EDL.[6,7] Recent experiments measured the slip length over a smooth liquid-solid interface to be around the order of nanometers.[8–10] Since the enhancement of a pressure-driven flow due to the slip is determined by the ratio of the slip length to the height of the channel,[11] nanometer slip length can only be effective for systems with nanometer length scales.

However, superhydrophobic surfaces covered with micro- or nanostructures effectively trapping bubbles[12,13] exhibit an apparent slip length of orders of microns.[14–17] The liquid moves over trapped bubbles, providing a means to reduce the friction.[18–20] Due to its large effective slip length, the superhydrophobic surface attracts many attentions and both experimental and numerical studies have been extensively carried out on pressure-driven flows over superhydrophobic surfaces.[21–30]

Accounting for the slip length of micrometers associated with superhydrophobic surfaces, such surfaces seem to have a promising future to improve the efficiency of energy-conversion microfluidic devices. But consider the anisotropic nature of superhydrophobic surfaces, the improvement is not obvious. In fact, recent studies on electro-osmotic flows over superhydrophobic surfaces are intriguing. For example, for uncharged liquid-gas interfaces, although the presence of bubbles reduces the friction, the amount of excess counterions inside the EDL also significantly decreases near the uncharged no-shear region. Therefore, the electro-osmotic flow induced by the action of an external electric field on excess counterions inside the EDL may not be inevitably enhanced by superhydrophobic surfaces. In fact, in the limits of thin EDLs and small zeta potentials, Squires[31] found out that an electro-osmotic flow over a superhydrophobic surface with uncharged liquid-gas interfaces is precisely the same as that over a homogeneously charged no-slip surface. Later, Bahga

[a)]Author to whom correspondence should be addressed. Electronic mail: hui.zhao@unlv.edu.

 © 2011 American Institute of Physics

Downloaded 13 Aug 2013 to 131.216.164.149. This article is copyrighted as indicated in the abstract. Reuse of AIP content is subject to the terms at: http://pof.aip.org/about/rights_and_permissions

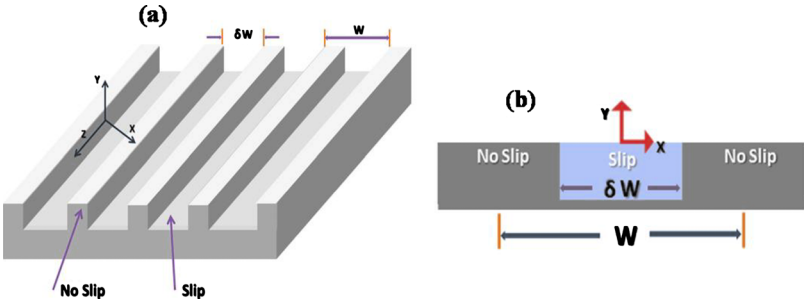

FIG. 1. (Color online) (a) A schematic of the geometry and the coordinate system. (b) The situation in (a) can be approximated by a periodic cell of size W.

et al.[32] reached the same conclusion using a different approach when the zeta potential is small. At moderate or large zeta potentials, the nonuniform surface conduction further decreases the electro-osmotic flow with uncharged liquid-gas interfaces which is smaller than its no-slip counterpart.[33] Flow enhancement likely happens with charged liquid-gas interfaces.[31–33]

Because the streaming potential results from the interaction of a pressure-driven flow and excess counterions inside the EDL, the interplay between the enhancement of the flow rate and the effect on excess counterions inside the EDL due to trapped bubbles should have an impact on the streaming potential. So far, this impact has not been reported in literature yet. One may speculate that according to the Onsager relation which directly relates the magnitude of electro-osmotic effect to that of the streaming current effect, the streaming current per pressure gradient is the same as the electro-osmotic mobility[1] and the streaming potential may be directly deduced from the electro-osmotic mobility. However, there is no general proof that the Onsager relation holds for superhydrophobic surfaces. Thus, for both fundamental and practical significance, it is worthwhile to examine the consequence of the slip on the streaming effect over superhydrophobic surfaces.

In this paper, we provide analytical solutions for the streaming potential over a charged superhydrophobic surface with an arbitrary double layer thickness in a thick channel and in the limit of small zeta potentials. In Sec. II, we derive expressions for the electric potential and the flow velocity by solving the Debye–Huckel and the Stokes equations, respectively. Next, formulas for the streaming current and streaming potential are presented in Sec. III. In Sec. IV, we discuss the effect of a superhydrophobic surface on the streaming potential in the limits of thin and thick EDLs, its implication for energy conversion and Onsager relation. Section V concludes.

II. MATHEMATICAL MODEL

Consider a pressure-driven flow in a rectangular channel containing periodically slip-stick stripes. The flow direction can be either longitudinal or transverse to the stripes. The size of the periodic cell is W. The width of the no-shear region is δW. The channel's height is $2H$. Here we assume $H \gg W$. In other words, we consider the case of a thick channel. The channel is filled with a 1-1 symmetric electrolyte with permittivity ε_1. Zeta potentials of no-slip and no-shear regions are, respectively, ζ_{NS} and ζ_S. Assume that the flow is fully developed. Here we assume that the liquid-gas interface is flat and no-shear. Detailed justification of these assumptions has been presented in Ybert *et al.*[30] Briefly, when surfaces with roughness are made of grooves (Fig. 1), and the viscosity of the gas is much smaller than that of the liquid, the curvature effect and the finite dissipation within the gas phase are not important.[30] We use the Cartesian coordinate (x,y) with its origin at the bottom of the channel. Figure 1 depicts the geometry and the coordinate system.

A. Electric potential

Electric double layers are developed near charged surfaces.[1,34,35] The electric potential (V) inside the EDL obeys the Poisson–Boltzmann equation. For a weakly charged surface ($\zeta \ll RT/F = 25$ mV at room temperature), the Poisson–Boltzmann equation can be further reduced to the Debye–Huckel equation,

$$\nabla^2 V = \kappa^2 V. \tag{1}$$

The boundary conditions are $V=\zeta_{\mathrm{NS}}$ on the liquid-solid interface and $V=\zeta_S$ on the liquid-gas interface. Above, all the variables are dimensionless. We use W as the length scale and RT/F as the electric potential scale. $\kappa = 1/\lambda_D = 1/W\sqrt{\varepsilon_1 RT/2FC_0}$, the inverse Debye screening length normalized with the length of the periodic cell W. C_0 is the solute's bulk concentration; R is the ideal gas constant; F is the Faraday constant; and T is the temperature.

Consider the periodic nature along the x direction $V(x,y)=V(x+1,y)$ and the symmetry with respect to $x=0$, one can expand V in a Fourier cosine series,

$$V(x,y) = \bar{\zeta} + \sum_{n=1}^{\infty} A_n(y)\cos(2n\pi x), \tag{2}$$

where $\bar{\zeta} = (1-\delta)\zeta_{\mathrm{NS}} + \delta\zeta_S$ is the average zeta potential. Equation (2) can be easily solved by separation of variables and yields[32]

$$V = \bar{\zeta}e^{-\kappa y} + \sum_{n=1}^{\infty} \frac{2(\zeta_S - \zeta_{\mathrm{NS}})\sin(n\pi\delta)}{n\pi} \times \cos(2n\pi x)e^{-\sqrt{\kappa^2+(2n\pi)^2}\,y}. \tag{3}$$

Downloaded 13 Aug 2013 to 131.216.164.149. This article is copyrighted as indicated in the abstract. Reuse of AIP content is subject to the terms at: http://pof.aip.org/about/rights_and_permissions

B. Hydrodynamics

1. Longitudinal stripes

Since the Reynolds number associated with microfluidic flows is typically small and the flow is fully developed, the axial velocity u satisfies the dimensionless Stokes equation,

$$\nabla^2 u = -2/H^2. \tag{4}$$

Above, the velocity is normalized by the maximum velocity occurring at the center of the channel. The velocity at the no-slip region obeys the no-slip condition ($u=0$) and the velocity at the no-shear region satisfies the perfect-slip condition ($\partial u/\partial y=0$). For convenience, u can be written as a superposition of the standard Poiseuille flow with no-slip walls and the correction due to the no-shear region,

$$u = 2\varepsilon y - (\varepsilon y)^2 + \hat{u}, \tag{5}$$

where $\varepsilon=1/H$. Similar to V, $\hat{u}$ can be again expanded as a Fourier cosine series,

$$\hat{u} = a_0 + \sum_{n=1}^{\infty} a_n \cos(2n\pi x) e^{-2n\pi y}. \tag{6}$$

The boundary conditions of $\hat{u}$ on the perfect-slip and no-slip regions become

$$2\varepsilon - \sum_{n=1}^{\infty} 2n\pi a_n \cos(2n\pi x) = 0, \quad 0 < x < \delta/2 \tag{7}$$

and

$$a_0 + \sum_{n=1}^{\infty} a_n \cos(2n\pi x) = 0, \quad \delta/2 < x < 1/2, \tag{8}$$

respectively. The above dual series can be solved exactly[29,36] to obtain

$$a_0 = \frac{2\varepsilon}{\pi} \ln\left(\sec\left(\frac{\delta\pi}{2}\right)\right) \tag{9}$$

and

$$a_n = \frac{\varepsilon}{\pi} \int_0^{\delta\pi} \tan(t/2)[P_n(\cos t) - P_{n-1}(\cos t)]dt, \tag{10}$$

where P_n is the nth order Legendre polynomial. The effective longitudinal slip length $\beta_\parallel$ deduced from the increase in the flow rate due to the slip is equal to $a_0/2(\beta_\parallel = a_0/2)$.

2. Transverse stripes

For transverse stripes, the pressure gradient depends on the axial variable x and it is convenient to define a streamfunction $\psi(x,y)$ by

$$u = \frac{\partial \psi}{\partial y}, \quad v = -\frac{\partial \psi}{\partial x}. \tag{11}$$

To facilitate the derivation, one can decompose this linear Stokes problem into a superposition of a parabolic flow and a perturbation to the parabolic flow,

$$\psi(x,y) = \psi_P(y) + \hat{\psi}(x,y), \quad \psi_P(y) = \varepsilon y^2 - \varepsilon^2 \frac{y^3}{3}. \tag{12}$$

The boundary conditions for $\hat{\psi}$ over the superhydrophobic surface are

$$\hat{\psi} = 0, \tag{13}$$

$$2\varepsilon + \frac{\partial^2 \hat{\psi}}{\partial y^2} = 0, \quad 0 < x < \delta/2, \tag{14}$$

and

$$\frac{\partial \hat{\psi}}{\partial y} = 0, \quad \delta/2 < x < 1/2. \tag{15}$$

To determine the streamfunction $\hat{\psi}$, we can first calculate the perturbation vorticity $\hat{\omega}$ since the streamfunction satisfies

$$\frac{\partial^2 \hat{\psi}}{\partial x^2} + \frac{\partial^2 \hat{\psi}}{\partial y^2} = \hat{\omega}. \tag{16}$$

The equation of the perturbation vorticity $\hat{\omega}$ can be obtained by taking the curl of the Stokes equation,

$$\frac{\partial^2 \hat{\omega}}{\partial x^2} + \frac{\partial^2 \hat{\omega}}{\partial y^2} = 0. \tag{17}$$

The solution of Eq. (17) can be found by using separation of variables,

$$\hat{\omega} = \sum_{n=1}^{\infty} c_n \cos(2n\pi x) e^{-2n\pi y}. \tag{18}$$

To derive Eq. (18), we have used the condition $\hat{\omega}$ is zero when $y \to \infty$.

With $\hat{\omega}$, the streamfunction $\hat{\psi}$ can thus be expressed as

$$\hat{\psi} = c_0 y + d_0 + \sum_{n=1}^{\infty} \cos(2n\pi x) f_n(y). \tag{19}$$

By substituting Eq. (19) into Eq. (16), one can obtain

$$f_n'' - (2n\pi)^2 f_n = c_n e^{-2n\pi y}. \tag{20}$$

The perturbation streamfunction $\hat{\psi}$ is therefore given by

$$\hat{\psi} = b_0 y + \sum_{n=1}^{\infty} b_n \cos(2n\pi x) y e^{-2n\pi y}. \tag{21}$$

Above, $b_n = -c_n/4n\pi$ and $b_0 = c_0$. To derive Eq. (21), we have used $\hat{\psi}=0$ at $y=0$, corresponding to $\hat{v}=0$, no penetration condition.

$\hat{u}$ can be written as

$$\hat{u} = \frac{\partial \hat{\psi}}{\partial y} = b_0 + \sum_{n=1}^{\infty} b_n \cos(2n\pi x)(1 - 2n\pi y) e^{-2n\pi y}. \tag{22}$$

The boundary conditions of $\hat{u}$ on the perfect-slip and no-slip regions become

Downloaded 13 Aug 2013 to 131.216.164.149. This article is copyrighted as indicated in the abstract. Reuse of AIP content is subject to the terms at: http://pof.aip.org/about/rights_and_permissions

$$2\varepsilon - \sum_{n=1}^{\infty} 4b_n n\pi \cos(2n\pi x) = 0, \quad \text{for } 0 < x < \delta/2 \tag{23}$$

and

$$b_0 + \sum_{n=1}^{\infty} b_n \cos(2n\pi x) = 0, \quad \text{for } \delta/2 < x < 1/2, \tag{24}$$

respectively. If we let $2b_n = a_n$, Eqs. (23) and (24) are identical to Eqs. (7) and (8). In other words, $b_n = a_n/2$. The effective transverse slip length $\beta_\perp$ deduced from the increase in the flow rate due to the slip is equal to $a_0/4$ or $\beta_\perp = \beta_\parallel/2$.[27]

III. STREAMING POTENTIAL

A superhydrophobic surface bears a zeta potential ζ_{NS} on the liquid-solid interface and ζ_S on the liquid-gas interface. Excess counterions inside the EDL are transported by a pressure-driven flow via convection. Such electroconvection forms an electric current termed streaming current.

A. Longitudinal stripes

The streaming current can be written as

$$J_S = 2\int_{y=0}^{\infty}\int_{x=0}^{x=1/2} \rho_e u dx dy, \tag{25}$$

where ρ_e, the charge density, is equal to $2/\kappa^2\nabla^2\psi$. In the case of the thick channel ($\varepsilon = 1/H \ll 1$), the higher order term $[(\varepsilon y)^2]$ in the velocity expression equation (5) can be neglected. Including Eqs. (3), (5), and (6) into Eq. (25) and accounting for the orthogonality of cosine functions, one can readily integrate Eq. (25) into a series,

$$J_{\parallel S} = \left(\frac{4}{\kappa^2}\varepsilon\bar{\zeta}(1+\kappa\beta_\parallel) + \sum_{n=1}^{\infty}\frac{2(\zeta_S - \zeta_{NS})\sin(n\delta\pi)}{n\pi}\frac{a_n}{2n\pi + \sqrt{\kappa^2 + (2n\pi)^2}}\right). \tag{26}$$

In the absence of an external electrical load, to maintain the conservation of the current, an electric potential (termed streaming potential) is built and generates a conduction current inside the channel. The electric field generated by the streaming potential can be written as $-\nabla\phi$. At steady state, to balance the streaming current, the streaming electric field has to satisfy

$$J_S - S\sigma\nabla\phi = 0. \tag{27}$$

Above, S is the area of the cross section and σ is the conductivity of the fluid. Here we neglect surface conduction over the superhydrophobic surface since the Dukhin number, characterizing the relative importance of surface conduction against the bulk conductivity, is much less than 1 when $\bar{\zeta} \ll 1$.

Finally, the streaming potential across the thick channel over a periodic cell can be readily derived from Eqs. (26) and (27),

$$\Delta\phi_\parallel = \frac{1}{S\sigma}\left(\frac{4}{\kappa^2}\varepsilon\bar{\zeta}(1+\kappa\beta_\parallel) + \sum_{n=1}^{\infty}\frac{2(\zeta_S - \zeta_{NS})\sin(n\delta\pi)}{n\pi}\frac{a_n}{2n\pi + \sqrt{\kappa^2 + (2n\pi)^2}}\right). \tag{28}$$

B. Transverse stripes

As pointed out in Brunet and Ajdari,[37] due to the anisotropic nature of the superhydrophobic surface, the streaming current is not uniform along the transverse stripes. A modulation of the streaming current along the axial direction results in current exchange with the bulk to maintain the charge conservation. Integrating along y alone is not sufficient to calculate the streaming potential. Instead, one can average the streaming current over one periodic cell to obtain a net response of the streaming potential to the pressure gradient.[37]

Including Eqs. (3), (5), and (22) into Eq. (25) and accounting for the orthogonality of cosine functions, again one can readily integrate Eq. (25) into a series,

$$J_{\perp S} = \left\{\frac{4}{\kappa^2}\varepsilon\bar{\zeta}(1+\kappa\beta_\perp) + \sum_{n=1}^{\infty}\frac{(\zeta_S - \zeta_{NS})\sin(n\delta\pi)}{n\pi}\frac{a_n\sqrt{\kappa^2 + (2n\pi)^2}}{[2n\pi + \sqrt{\kappa^2 + (2n\pi)^2}]^2}\right\}. \tag{29}$$

The net streaming potential over a periodic cell becomes

$$\Delta\phi_\perp = \frac{1}{S\sigma}\left\{\frac{4}{\kappa^2}\varepsilon\bar{\zeta}(1+\kappa\beta_\perp) + \sum_{n=1}^{\infty}\frac{(\zeta_S - \zeta_{NS})\sin(n\delta\pi)}{n\pi}\frac{a_n\sqrt{\kappa^2 + (2n\pi)^2}}{[2n\pi + \sqrt{\kappa^2 + (2n\pi)^2}]^2}\right\}. \tag{30}$$

IV. DISCUSSIONS

To understand the role of the slip, the streaming potential equations (28) and (30) are compared against that over a uniformly charged no-slip surface bearing the zeta potential ζ_{NS}, which is equal to

$$\Delta\phi_{NS} = \frac{4}{S\sigma\kappa^2}\varepsilon\zeta_{NS}. \tag{31}$$

The ratio of Eq. (28) to Eq. (31) defined as $\alpha_\parallel$ characterizing the possible enhancement of the streaming potential over a longitudinal superhydrophobic surface is

Downloaded 13 Aug 2013 to 131.216.164.149. This article is copyrighted as indicated in the abstract. Reuse of AIP content is subject to the terms at: http://pof.aip.org/about/rights_and_permissions

$$\alpha_{\parallel} = \left(\frac{\bar{\zeta}}{\zeta_{\mathrm{NS}}}(1+\kappa\beta_{\parallel}) + \kappa^2 \sum_{n=1}^{\infty} \frac{(\zeta_S/\zeta_{\mathrm{NS}}-1)\sin(n\delta\pi)}{2n\pi} \frac{a_n}{2n\pi+\sqrt{\kappa^2+(2n\pi)^2}} \right). \tag{32}$$

The ratio of Eq. (30) to Eq. (31), $\alpha_{\perp}$, is

$$\alpha_{\perp} = \left\{ \frac{\bar{\zeta}}{\zeta_{\mathrm{NS}}}(1+\kappa\beta_{\perp}) + \kappa^2 \sum_{n=1}^{\infty} \frac{(\zeta_S/\zeta_{\mathrm{NS}}-1)\sin(n\delta\pi)}{4n\pi} \frac{a_n\sqrt{\kappa^2+(2n\pi)^2}}{[2n\pi+\sqrt{\kappa^2+(2n\pi)^2}]^2} \right\}. \tag{33}$$

A. Thin electric double layer limit

In the thin-EDL limit ($\kappa \to \infty$), Eq. (32) can be further reduced. The terms in Eq. (32) can be expanded in terms of $1/\kappa$,

$$\frac{a_n}{2n\pi+\sqrt{\kappa^2+(2n\pi)^2}} = \frac{a_n}{\kappa}\left(1-\frac{2n\pi}{\kappa}\right) + O\left[\left(\frac{1}{\kappa}\right)^2\right]. \tag{34}$$

Substituting Eq. (34) into Eq. (32), we have

$$\alpha_{\parallel} = \frac{\bar{\zeta}}{\zeta_{\mathrm{NS}}}(1+\kappa\beta_{\parallel}) + (\zeta_S/\zeta_{\mathrm{NS}}-1) \times \sum_{n=1}^{\infty} \left(\kappa \frac{\sin(n\delta\pi)}{2n\pi} a_n - \sin(n\delta\pi) a_n \right). \tag{35}$$

To evaluate Eq. (35), one can integrate Eq. (7) from 0 to $\delta/2$ and Eq. (8) from $\delta/2$ to 1/2, respectively,

$$\sum_{n=1}^{\infty} \sin(n\delta\pi) a_n = \varepsilon\delta \tag{36}$$

and

$$\sum_{n=1}^{\infty} \frac{\sin(n\delta\pi)}{n\pi} a_n = (1-\delta) a_0. \tag{37}$$

Substituting Eqs. (36) and (37) into Eq. (35), replacing $\bar{\zeta}=(1-\delta)\zeta_{\mathrm{NS}}+\delta\zeta_S$, and after some algebraic derivation, one obtains

$$\alpha_{\parallel} = 1 + \beta_{\parallel}\kappa\frac{\zeta_S}{\zeta_{\mathrm{NS}}}. \tag{38}$$

Similarly, the transverse enhancement ratio $\alpha_{\perp}$ can also be reduced at the thin-EDL limit ($\kappa \to \infty$). The terms in Eq. (33) can be expanded in terms of $1/\kappa$ as well,

$$\frac{a_n\sqrt{\kappa^2+(2n\pi)^2}}{[2n\pi+\sqrt{\kappa^2+(2n\pi)^2}]^2} = \frac{a_n}{\kappa}\left(1-2\frac{2n\pi}{\kappa}\right) + O\left[\left(\frac{1}{\kappa}\right)^2\right]. \tag{39}$$

Then Eq. (33) becomes

$$a_{\perp} = \frac{\bar{\zeta}}{\zeta_{\mathrm{NS}}}(1+\kappa\beta_{\perp}) + (\zeta_S/\zeta_{\mathrm{NS}}-1) \times \sum_{n=1}^{\infty} \left(\frac{\sin(n\delta\pi)}{4n\pi} \kappa a_n - \sin(n\delta\pi) a_n \right). \tag{40}$$

Substituting Eqs. (36) and (37) into Eq. (40), replacing $\bar{\zeta}=(1-\delta)\zeta_{\mathrm{NS}}+\delta\zeta_S$, and considering $\beta_{\perp}=a_0/4$, one obtains

$$\alpha_{\perp} = 1 + \beta_{\perp}\kappa\frac{\zeta_S}{\zeta_{\mathrm{NS}}}. \tag{41}$$

Equations (38) and (41) are exactly the same as the enhancement ratio of the electro-osmotic mobility over a superhydrophobic surface to that over a homogeneously charged no-slip surface (see also the Appendix).[31,32] Notice that $\beta_{\parallel}=2\beta_{\perp}$. The enhancement ratio of the streaming potential is different for longitudinal and transverse stripes. Similar to the hydrodynamic slip over a superhydrophobic surface,[21] in general α is a tensor. The enhancement depends on the orientation of the stripped pattern.

For uncharged liquid-gas interfaces ($\zeta_S=0$), Eqs. (38) and (41) are both equal to 1. There is no enhancement of the streaming potential due to the slip. In other words, the streaming potential is precisely the same as that over a homogeneously charged no-slip surface, regardless of the area fraction of the no-shear region (δ). As pointed out before, the streaming potential is generated by the interaction of a pressure-driven flow and excess ions inside the EDL. On one hand, the superhydrophobic surface boosts the flow rate, attempting to increase the streaming potential. On the other hand, the uncharged liquid-gas interface reduces the amount of excess ions inside the EDL, leading to a decrease of the streaming potential. In the thin-EDL limit, apparently the loss of the streaming potential over a superhydrophobic surface owing to the uncharged liquid-gas interface exactly cancels out the gain of the streaming potential by the increase of the flow rate. Similarly, there is also no enhancement of electro-osmotic flows over superhydrophobic surfaces with uncharged liquid-gas interfaces.[31,32]

B. Thick electric double layer limit

We now turn to the opposite limit: thick EDLs, where $\kappa \to \infty$. In the case of thick EDLs, one can immediately neglect the terms containing higher order κ in Eqs. (32) and (33) and have

$$\alpha_{\parallel,\perp} = \frac{\bar{\zeta}}{\zeta_{\mathrm{NS}}}(1+\kappa\beta_{\parallel,\perp}). \tag{42}$$

Again Eq. (42) is precisely the same as the electro-osmotic mobility over a superhydrophobic surface in the thick-EDL limit (Appendix).[32]

C. Charged liquid-gas interface

Equations (38) and (41) indicate that in the limit of thin EDLs the increase of the streaming potential due to the slip is only observed when the liquid-gas interface is charged. There are experimental evidences and molecular dynamic

Downloaded 13 Aug 2013 to 131.216.164.149. This article is copyrighted as indicated in the abstract. Reuse of AIP content is subject to the terms at: http://pof.aip.org/about/rights_and_permissions

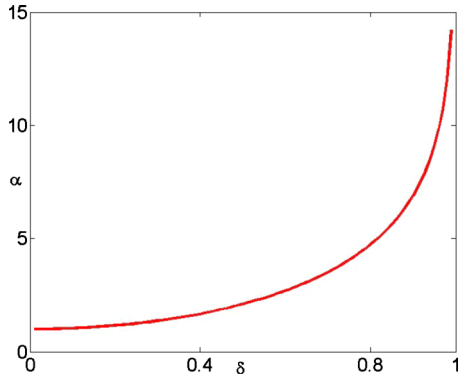

FIG. 2. (Color online) α as a function of δ for longitudinal stripes when $\kappa=100$, $\zeta_S/\zeta_{NS}=0.1$, and $\zeta_{NS}=-0.1$.

simulations supporting that the water-air interface is negatively charged due to excess OH^-.[38,39] The zeta potential of a water-air interface was measured to be in the range of -30 to -65 mV.[40–44]

For a uniformly charged surface $\zeta_{NS}=\zeta_S$, a simple expression can be immediately obtained from Eqs. (32) and (33) for an arbitrary EDL length,

$$\alpha_{\parallel,\perp} = 1 + \kappa\beta_{\parallel,\perp}. \tag{43}$$

This result indicates that when the zeta potential is constant over the entire surface, the streaming potential is given by the same formula assuming that the surface has an isotropic slip length β.[45,46] The streaming potential does not depend on the specific nature of the structure of the superhydrophobic surface as long as the surface is uniformly charged and has the same effective slip length β. It is readily explained: when the surface is uniformly charged, only the hydrodynamic flow makes a difference in the streaming potential. When each surface has the same effective slip length, the enhancement of the flow rate stays the same and so does the streaming potential.

When the charge distribution is not homogeneous, the enhancement of the streaming potential is still likely. Particularly, in the limit of thin EDLs, such enhancement can be remarkable. Figure 2 depicts $\alpha_\parallel$ as a function of δ for longitudinal stripes when $\kappa=100$, $\zeta_S/\zeta_{NS}=0.1$, and $\zeta_{NS}=-0.1$. Figure 2 suggests that with charged liquid-gas interfaces the enhancement can be observed. Even when $|\zeta_S|<|\zeta_{NS}|$, the streaming potential can still be significantly enhanced by increasing the area fraction of the liquid-gas interface (δ).

To examine the effect of double layer thickness on the enhancement of the streaming potential, Figs. 3 and 4 respectively plot α as a function of κ: $\zeta_S/\zeta_{NS}=0.5$ (dotted-dashed line), $\zeta_S/\zeta_{NS}=1$ (dashed line), and $\zeta_S/\zeta_{NS}=2$ (solid line) for longitudinal stripes and transverse stripes when $\delta=1/2$ and $\zeta_{NS}=-0.1$. In Figs. 3(a) and 4(a) the liquid-gas interface is uncharged. As the double layer thickness decreases (κ increases), α asymptotically increases from its thick-EDL limit (0.5) to its thin-EDL limit (1). For charged liquid-gas interfaces, the enhancement is still possible for a broad range of double layer thickness.

Both Figs. 3 and 4 suggest that the enhancement due to the slip decreases as the double layer thickness increases. In

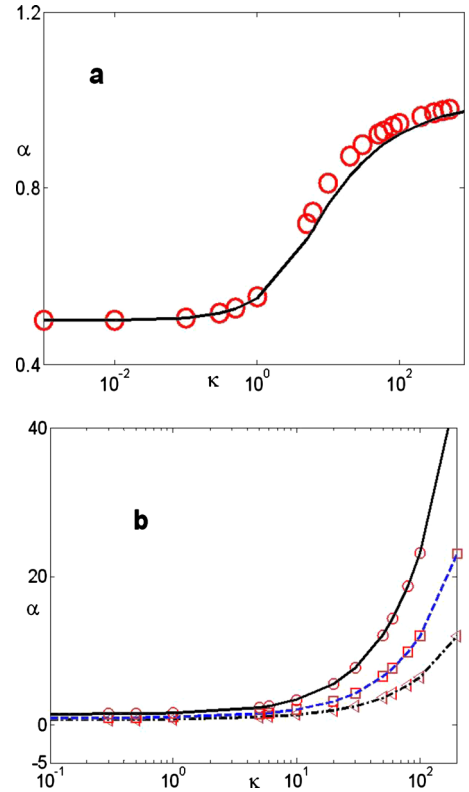

FIG. 3. (Color online) α as a function of κ for longitudinal stripes. (a) $\zeta_S/\zeta_{SN}=0$; (b) $\zeta_S/\zeta_{NS}=0.5$ (dotted-dashed line), $\zeta_S/\zeta_{NS}=1$ (dashed line), and $\zeta_S/\zeta_{NS}=2$ (solid line); when $\delta=1/2$ and $\zeta_{NS}=-0.1$. The lines and symbols correspond, respectively, to the enhancement ratios of streaming potential and electro-osmotic mobility due to the slip.

particular, when the double layer thickness $(1/\kappa)$ is larger than the slip length β, the enhancement of the streaming potential is only possible when the zeta potential of the liquid-gas interface is comparable to that of the liquid-solid interface. It can be explained: when the slip length is smaller than the double layer thickness, excess counterions contributing to the streaming current spread out in a much larger region where the hydrodynamic slip has only a marginal impact, while the less charged liquid-gas interface decreases the charge density within the double layer, leading to a smaller streaming current. Therefore, it is not surprising that the enhancement of the streaming potential can be lost in thick EDLs even for certain charged liquid-gas interfaces.

D. The Onsager relation

The Onsager relation predicts that the streaming current per ∇p is the same as the electro-osmotic mobility for a linear electrohydrodynamic response.[1,47] Under the thin double layer assumption, the Onsager relation was proved to be valid for complex geometries with nonslip surfaces and arbitrary zeta potential distribution.[37] However, there is no general proof for an arbitrary double layer thickness and an anisotropic slip condition. Interestingly, Eqs. (38) and (41)–(43) are the same as the enhancement ratio of the electro-osmotic mobility over superhydrophobic surfaces,[32] proving that the Onsager relation holds for thin and thick EDLs and

Downloaded 13 Aug 2013 to 131.216.164.149. This article is copyrighted as indicated in the abstract. Reuse of AIP content is subject to the terms at: http://pof.aip.org/about/rights_and_permissions

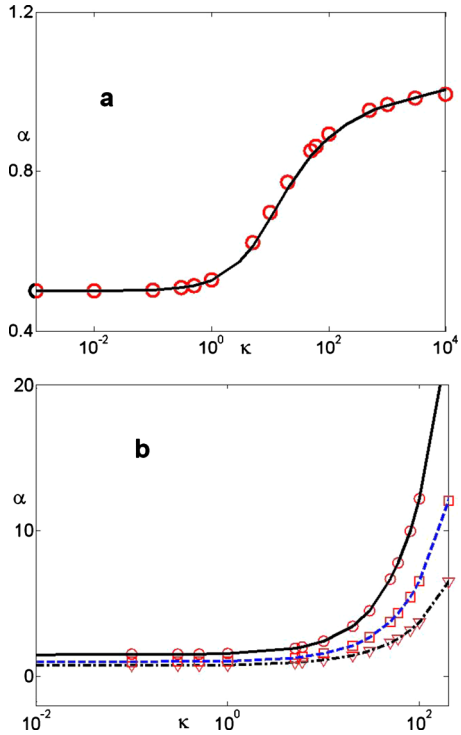

FIG. 4. (Color online) α as a function of κ for transverse stripes. (a) $\zeta_S/\zeta_{NS}=0$; (b) $\zeta_S/\zeta_{NS}=0.5$ (dotted-dashed line), $\zeta_S/\zeta_{NS}=1$ (dashed line), and $\zeta_S/\zeta_{NS}=2$ (solid line); when $\delta=1/2$ and $\zeta_{NS}=-0.1$. The lines and symbols correspond, respectively, to the enhancement ratios of streaming potential and electro-osmotic mobility due to the slip.

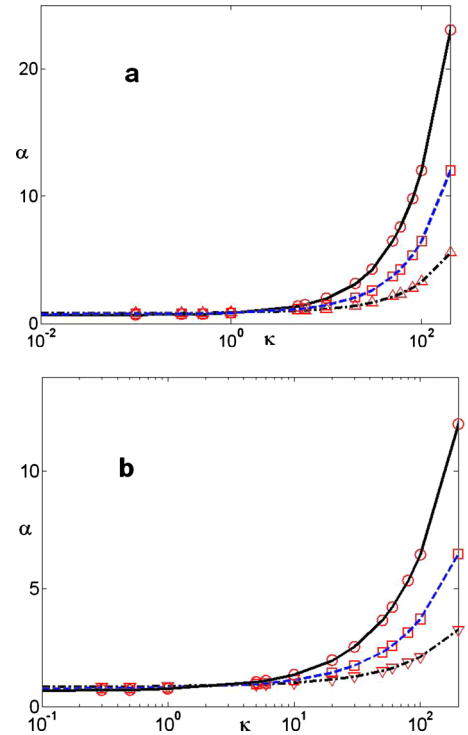

FIG. 5. (Color online) α as a function of κ for $\delta=2/3$ (solid line), $\delta=1/2$ (dashed line), and $\delta=1/3$ (dotted-dashed line); when $\zeta_S/\zeta_{NS}=0.5$ and $\zeta_{NS}=-0.1$. (a) Longitudinal stripes. (b) Transverse stripes. The lines and symbols correspond, respectively, to the enhancement ratios of streaming potential and electro-osmotic mobility due to the slip.

homogeneously charged surfaces. However, we still cannot strictly prove that in general the Onsager relation is valid for superhydrophobic surfaces.

Instead, we compared the enhancement ratio of the streaming potential to its counterpart of the electro-osmotic mobility for various conditions. In Figs. 3 and 4, the lines and symbols correspond, respectively, to the enhancement ratios of streaming potential and electro-osmotic mobility due to the slip. Figure 5 depicts the enhancement ratio α as a function of κ for different area fraction of the liquid-gas interface δ for both longitudinal [Fig. 5(a)] and transverse stripes [Fig. 5(b)]. Again the lines and symbols correspond, respectively, to the enhancement ratios of streaming potential and electro-osmotic mobility due to the slip. The excellent agreement between these two ratios suggests that the Onsager relation appears to be valid for an arbitrary double layer thickness despite that we cannot prove it. The results are remarkable since it appears that the Onsager relation can be extended to a superhydrophobic surface for an arbitrary double layer thickness.

V. CONCLUSION

We analyzed the streaming potential over a patterned superhydrophobic surface with periodically distributed regions of no-shear and no-slip in the limit of small zeta potentials. We derived a general solution for an arbitrary EDL thickness and an area fraction of the no-shear region for both longitudinal and transverse stripes. In the limits of thin and thick EDLs, simple expressions were also given. The interplay between the enhancement of the flow rate and the effect on excess counterions inside the EDL due to trapped bubbles determines the magnitude of the streaming potential. In general, the enhancement ratio α is a tensor. The enhancement depends on the orientation of the stripped pattern. Our main conclusion is that in contrast to the case of the flow rate the enhancement of the streaming potential over a superhydrophobic surface is only possible under certain conditions.

When the liquid-gas interface is uncharged, the streaming potential over a superhydrophobic surface is smaller than or equal to that over a uniformly charged no-slip surface bearing the same zeta potential. On the contrary, for a uniformly charged superhydrophobic surface, the streaming potential can be possibly enhanced by several orders of magnitude, suggesting that a novel fluidic system exploring superhydrophobic surfaces with applications to energy conversion is only feasible with charged liquid-gas interfaces. Furthermore, the enhancement decreases as the double layer thickness increases. For a less charged liquid-gas interface, the enhancement can be lost at thick EDLs.

Under the assumption of small zeta potentials, the Onsager relation which directly relates the magnitude of electro-osmotic effect to that of the streaming current effect was explicitly proved to be valid for thin and thick EDLs and a homogeneously charged superhydrophobic surface. With respect to an arbitrary double layer thickness, the enhancement ratio of the streaming potential was compared against the ratio of the electro-osmotic mobility computed numerically for different area fraction of the liquid-gas interface and

Downloaded 13 Aug 2013 to 131.216.164.149. This article is copyrighted as indicated in the abstract. Reuse of AIP content is subject to the terms at: http://pof.aip.org/about/rights_and_permissions

ζ_S/ζ_{NS}. The excellent agreements between these two ratios indicated that the Onsager relation seems to be applicable for arbitrary superhydrophobic surfaces. This conclusion is useful since one can directly extend the results of the streaming current to the electro-osmotic mobility or vice verse.

Here we assumed that the zeta potential of the entire surface is much smaller than the thermal potential so that the Debye–Huckel approximation can be applied. In the limit of small zeta potentials, surface conduction is negligible. When the surface is moderately or highly charged, the surface conduction may play a role and complicate the streaming potential even with uncharged liquid-gas interfaces. At moderate or large zeta potentials, it is generally true that the streaming current with uncharged liquid-gas interfaces is smaller than that over a homogeneously charged no-slip surface. But σ in Eq. (27) consisting of both bulk conductivity and surface conduction of a superhydrophobic surface is also smaller than that over a no-slip surface since the uncharged liquid-gas interface yields almost zero surface conduction over the no-shear region. Notice that the streaming potential, proportional to $1/\sigma$, is not solely determined by the streaming current any more. Such effect of surface conduction on the streaming potential may deserve further attention and certainly is in order for future consideration.

APPENDIX: THE ELECTRO-OSMOTIC MOBILITY OVER TRANSVERSE STRIPES

In this appendix, we present a detailed derivation of the enhancement ratio of the electro-osmotic mobility over transverse stripes. For transverse stripes, the pressure gradient depends on the axial variable x and it is convenient to define a streamfunction $\psi(x,y)$ by

$$u = \frac{\partial \psi}{\partial y}, \quad v = -\frac{\partial \psi}{\partial x}. \tag{A1}$$

Above, the velocity scale is $\varepsilon E_0 RT/\mu F$ where E_0 is the external electric field.

To determine the streamfunction ψ, we can first calculate the vorticity ω since the streamfunction ψ satisfies

$$\nabla^2 \psi = \omega. \tag{A2}$$

The vorticity obeys the following equation:

$$\nabla^2 \omega = \kappa^2 \frac{\partial V}{\partial y}. \tag{A3}$$

Thus,

$$\nabla^4 \psi = \kappa^2 \frac{\partial V}{\partial y}. \tag{A4}$$

The general solution is

$$\psi = c_0 + u_0 y + \sum_{n=1}^{\infty} \cos(2n\pi x)(P_n e^{-2n\pi y} + Q_n y e^{-2n\pi y}) + \frac{1}{\kappa^2}\frac{\partial V}{\partial y}. \tag{A5}$$

Since $\psi=0$ at $y=0$, we have

$$\psi = c_0 + \sum_{n=1}^{\infty} P_n \cos(2n\pi x) - \frac{\bar{\zeta}}{\kappa} - \frac{1}{\kappa^2}\sum_{n=1}^{\infty} \sqrt{\kappa^2 + (2n\pi)^2} B_n \cos(2n\pi x) = 0. \tag{A6}$$

Thus, $P_n = \sqrt{\kappa^2 + (2n\pi)^2} B_n/\kappa^2$ where $B_n = 2(\zeta_S - \zeta_{NS}) \times \sin(n\pi\delta)/n\pi$. The axial velocity is

$$u = \frac{\partial \psi}{\partial y} = u_0 + \sum_{n=1}^{\infty} \cos(2n\pi x) \times [-P_n 2n\pi e^{-2n\pi y} + Q_n(e^{-2n\pi y} - 2n\pi y e^{-2n\pi y})] + \frac{1}{\kappa^2}\frac{\partial^2 V}{\partial y^2} \tag{A7}$$

or

$$u = \frac{\partial \psi}{\partial y} = u_0 + \sum_{n=1}^{\infty} \left(-P_n 2n\pi e^{-2n\pi y} + Q_n(e^{-2n\pi y} - 2n\pi y e^{-2n\pi y}) + \left\{ \frac{[(2n\pi)^2 + \kappa^2] B_n e^{-\sqrt{(2n\pi)^2+\kappa^2} y}}{\kappa^2} \right\} \right) \times \cos(2n\pi x) + \bar{\zeta} e^{-\kappa y}. \tag{A8}$$

On the superhydrophobic surface,

$$\sum_{n=1}^{\infty} \cos(2n\pi x)[-\sqrt{(2n\pi)^2 + \kappa^2} B_n + Q_n(-4n\pi)] - \kappa\bar{\zeta} = 0, \quad 0 < x < \delta/2 \tag{A9}$$

and

$$u_0 + \sum_{n=1}^{\infty} \cos(2n\pi x) \left\{ -\frac{2n\pi\sqrt{\kappa^2 + (2n\pi)^2} B_n}{\kappa^2} + Q_n + \frac{[(2n\pi)^2 + \kappa^2] B_n}{\kappa^2} \right\} + \bar{\zeta} = 0, \quad \delta/2 < x < 1/2. \tag{A10}$$

At the thin-EDL limits ($\kappa \to \infty$), $2n\pi/\kappa \to 0$, and $\sqrt{(2n\pi^2 + \kappa^2)}/\kappa \to 1$, Eqs. (A9) and (A10) become

$$\sum_{n=1}^{\infty} -4n\pi Q_n \cos(\lambda_n x) - \kappa\zeta_S = 0, \quad 0 < x < \delta/2 \tag{A11}$$

and

$$u_0 + \sum_{n=1}^{\infty} Q_n \cos(\lambda_n x) + \zeta_{NS} = 0, \quad \delta/2 < x < 1/2, \tag{A12}$$

since $\zeta = \bar{\zeta} + \Sigma_{n=1}^{\infty} B_n \cos(\lambda_n x)$. Equations (A11) and (A12) can be readily integrated,[36]

$$u_0 + \zeta_{NS} = -\beta_\perp \kappa \zeta_S, \tag{A13}$$

or M_E, the enhancement ratio of the electro-osmotic mobility due to the slip, is

Downloaded 13 Aug 2013 to 131.216.164.149. This article is copyrighted as indicated in the abstract. Reuse of AIP content is subject to the terms at: http://pof.aip.org/about/rights_and_permissions

$$M_E = \frac{u_0}{-\zeta_{\mathrm{NS}}} = 1 + \kappa\beta_\perp \frac{\zeta_S}{\zeta_{\mathrm{NS}}}. \tag{A14}$$

In the limit of thick EDLs, $\kappa \to 0$.

The terms in Eq. (A10) can be expanded in terms of κ,

$$\begin{aligned} &-\frac{2n\pi\sqrt{\kappa^2+(2n\pi)^2}B_n}{\kappa^2} + \frac{[(2n\pi)^2+\kappa^2]B_n}{\kappa^2} \\ &= \sqrt{(2n\pi)^2+\kappa^2}\left[\sqrt{(2n\pi)^2+\kappa^2} - 2n\pi\right]\frac{B_n}{\kappa^2} \\ &= \frac{\sqrt{(2n\pi)^2+\kappa^2}B_n}{\kappa^2} 2n\pi\left[\sqrt{1+\left(\frac{\kappa}{2n\pi}\right)^2} - 1\right] \\ &= \frac{\sqrt{(2n\pi)^2+\kappa^2}B_n}{\kappa^2} 2n\pi \frac{1}{2}\left(\frac{\kappa}{2n\pi}\right)^2 + o(\kappa^3). \end{aligned} \tag{A15}$$

When $\kappa \to 0$, $\sqrt{(2n\pi)^2+\kappa^2}/2n\pi \to 1$. Thus, Eq. (A10) becomes

$$u_0 + \sum_{n=1}^{\infty} \cos(\lambda_n x)\left(Q_n + \frac{B_n}{2}\right) + \bar{\zeta} = 0. \tag{A16}$$

Equation (A9) can be changed to

$$\sum_{n=1}^{\infty} -4n\pi \cos(2n\pi x)\left(Q_n + \frac{B_n}{2}\right) - \kappa\bar{\zeta} = 0. \tag{A17}$$

Therefore, Eqs. (A16) and (A17) can be readily solved,

$$M_E = \frac{\bar{\zeta}}{\zeta_{\mathrm{NS}}}(1 + \kappa\beta_\perp). \tag{A18}$$

For an arbitrary κ, Eqs. (A9) and (A10) have to be solved numerically to compute M_E. To calculate coefficients Q_n, we truncate the dual series equations at Q_{N-1}, multiple $\cos 2m\pi x (m < N)$ with Eqs. (A9) and (A10), and integrate them along their respective domains. The resulting linear system is then solved and the solution converges upon truncation refinement.

[1] J. Lyklema, *Fundamentals of Interface and Colloid Science. Volume II: Solid-Liquid Interfaces* (Academic, San Diego, 1995).
[2] F. A. Morrison and J. F. Osterle, "Electrokinetic energy conversion in ultrafine capillaries," J. Chem. Phys. **43**, 2111 (1965).
[3] F. H. J. van der Heyden, D. Stein, and C. Dekker, "Streaming currents in a single nanofluidic channel," Phys. Rev. Lett. **95**, 116104 (2005).
[4] F. H. J. van der Heyden, D. J. Bonthuis, D. Stein, C. Meyer, and C. Dekker, "Electrokinetic energy conversion efficiency in nanofluidic channels," Nano Lett. **6**, 2232 (2006).
[5] F. H. J. van der Heyden, D. J. Bonthuis, D. Stein, C. Meyer, and C. Dekker, "Power generation by pressure-driven transport of ions in nanofluidic channels," Nano Lett. **7**, 1022 (2007).
[6] S. Pennathur, J. C. T. Eikel, and A. van den Berg, "Energy conversion in microsystems: Is there a role for micro/nanofluidics?," Lab Chip **7**, 1234 (2007).
[7] Y. Ren and D. Stein, "Slip-enhanced electrokinetic energy conversion in nanofluidic channels," Nanotechnology **19**, 195707 (2008).
[8] O. I. Vinogradova, "Slippage of water over hydrophobic surfaces," Int. J. Min. Process. **56**, 31 (1999).
[9] C. Neto, D. R. Evans, E. Bonaccurso, H. J. Butt, and V. S. J. Craig, "Boundary slip in Newtonian liquids: A review of experimental studies," Rep. Prog. Phys. **68**, 2859 (2005).
[10] E. Lauga, M. P. Brenner, and H. A. Stone, in *Handbook of Experimental Fluid Dynamics*, edited by C. Tropea, A. Yarin, and J. F. Foss (Springer, New York, 2007), pp. 1219–1240.
[11] O. I. Vinogradova, "Drainage of thin liquid-film confined between hydrophobic surfaces," Langmuir **11**, 2213 (1995).
[12] L. Bocquet and J. L. Barrat, "Flow boundary conditions from nano- to micro-scales," Soft Matter **3**, 685 (2007).
[13] J. P. Rothstein, "Slip on superhydrophobic surfaces," Annu. Rev. Fluid Mech. **42**, 89 (2010).
[14] C. H. Choi and C. J. Kim, "Large slip of aqueous liquid flow over a nanoengineered superhydrophobic surface," Phys. Rev. Lett. **96**, 066001 (2006).
[15] C. Lee, C. H. Choi, and C. J. Kim, "Structured surfaces for a giant liquid slip," Phys. Rev. Lett. **101**, 064501 (2008).
[16] J. Ou and J. P. Rothstein, "Direct velocity measurements of the flow past drag-reducing ultrahydrophobic surfaces," Phys. Fluids **17**, 103606 (2005).
[17] P. C. Tsai, A. M. Peters, C. Pirat, M. Wessling, R. G. H. Lammertink, and D. Lohse, "Quantifying effective slip length over micropatterned hydrophobic surfaces," Phys. Fluids **21**, 112002 (2009).
[18] C. Cottin-Bizonne, J.-L. Barrat, L. Bocquet, and E. Charlaix, "Low-friction flows of liquid at nanopatterned interfaces," Nature Mater. **2**, 237 (2003).
[19] J. Ou, B. Perot, and J. P. Rothstein, "Laminar drag reduction in microchannels using ultrahydrophobic surfaces," Phys. Fluids **16**, 4635 (2004).
[20] C. H. Choi, U. Ulmanella, J. Kim, C. M. Ho, and C. J. Kim, "Effective slip and friction reduction in nanograted superhydrophobic microchannels," Phys. Fluids **18**, 087105 (2006).
[21] M. Z. Bazant and O. I. Vinogradova, "Tensorial hydrodynamic slip," J. Fluid Mech. **613**, 125 (2008).
[22] A. V. Belyaev and O. I. Vinogradova, "Effective slip in pressure-driven flow past super-hydrophobic stripes," J. Fluid Mech. **652**, 489 (2010).
[23] J. Davies, D. Maynes, B. W. Webb, and B. Woolford, "Laminar flow in a microchannel with superhydrophobic walls exhibiting transverse ribs," Phys. Fluids **18**, 087110 (2006).
[24] F. Feuillebois, M. Z. Bazant, and O. I. Vinogradova, "Effective slip over superhydrophobic surfaces in thin channels," Phys. Rev. Lett. **102**, 026001 (2009).
[25] P. Gao and J. J. Feng, "Enhanced slip on a patterned substrate due to depinning of contact line," Phys. Fluids **21**, 102102 (2009).
[26] P. Joseph, C. Cottin-Bizonne, J. M. Benoit, C. Ybert, C. Journet, P. Tabeling, and L. Bocquet, "Slippage of water past superhydrophobic carbon nanotube forests in microchannels," Phys. Rev. Lett. **97**, 156104 (2006).
[27] E. Lauga and H. A. Stone, "Effective slip in pressure-driven flow," J. Fluid Mech. **489**, 55 (2003).
[28] D. Maynes, K. Jeffs, B. Woolford, and B. W. Webb, "Laminar flow in a microchannel with hydrophobic surface patterned microribs oriented parallel to the flow direction," Phys. Fluids **19**, 093603 (2007).
[29] M. Sbragaglia and A. Prosperetti, "A note on the effective slip properties for microchannel flows with ultrahydrophobic surfaces," Phys. Fluids **19**, 043603 (2007).
[30] C. Ybert, C. Barentin, C. Cottin-Bizonne, P. Joseph, and L. Bocquet, "Achieving large slip with superhydrophobic surfaces: Scaling laws for generic geometries," Phys. Fluids **19**, 123601 (2007).
[31] T. M. Squires, "Electrokinetic flows over inhomogeneously slipping surfaces," Phys. Fluids **20**, 092105 (2008).
[32] S. S. Bahga, O. I. Vinogradova, and M. Z. Bazant, "Anisotropic electro-osmotic flow over super-hydrophobic surfaces," J. Fluid Mech. **644**, 245 (2010).
[33] H. Zhao, "Electro-osmotic flow over a charged superhydrophobic surface," Phys. Rev. E **81**, 066314 (2010).
[34] R. J. Hunter, *Foundations of Colloid Science* (Oxford University Press, New York, 2001).
[35] R. J. Hunter, *Zeta Potential in Colloid Science: Principles and Applications* (Academic, San Diego, 1981).
[36] I. N. Sneddon, *Mixed Boundary Value Problems in Potential Theory* (North-Holland, Amsterdam, 1966).
[37] E. Brunet and A. Ajdari, "Thin double layer approximation to describe streaming current fields in complex geometries: Analytical framework and applications to microfluidics," Phys. Rev. E **73**, 056306 (2006).
[38] M. Takahashi, "Zeta potential of microbubbles in aqueous solutions: Electric properties of the gas-water interface," J. Phys. Chem. B **109**, 21858 (2005).
[39] R. Zangi and J. B. F. N. Engberts, "Physisorption of hydroxide ions from aqueous solution to a hydrophobic surface," J. Am. Chem. Soc. **127**, 2272 (2005).

Downloaded 13 Aug 2013 to 131.216.164.149. This article is copyrighted as indicated in the abstract. Reuse of AIP content is subject to the terms at: http://pof.aip.org/about/rights_and_permissions

[40]A. Graciaa, G. Morel, P. Saulner, J. Lachaise, and R. S. Schechter, "The zeta potential of gas-bubbles," J. Colloid Interface Sci. **172**, 131 (1995).
[41]J. S. H. Lee, I. Barbulovic-Nad, Z. Wu, X. Xuan, and D. Li, "Electrokinetic flow in a free surface-guided microchannel," J. Appl. Phys. **99**, 054905 (2006).
[42]C. Yang, T. Dabros, D. Li, J. Czarnecki, and J. H. Masliyah, "Measurement of the zeta potential of gas bubbles in aqueous solutions by microelectrophoresis method," J. Colloid Interface Sci. **243**, 128 (2001).
[43]F. Y. Ushikubo, T. Furukawa, R. Nakagawa, M. Enari, Y. Makino, Y. Kawagoe, T. Shilina, and S. Oshita, "Evidence of the existence and the stability of nano-bubbles in water," Colloids Surf., A **361**, 31 (2010).
[44]F. Jin, J. F. Li, X. D. Ye, and C. Wu, "Effects of pH and ionic strength on the stability of nanobubbles in aqueous solutions of alpha-cyclodextrin," J. Phys. Chem. B **111**, 11745 (2007).
[45]V. M. Muller, I. P. Sergeeva, V. D. Sobolev, and N. V. Churaev, "Boundary effects in the theory of electrokinetic phenomena," Colloid J. USSR **48**, 606 (1986).
[46]L. Joly, C. Ybert, E. Trizac, and L. Bocquet, "Hydrodynamics within the electric double layer on slipping surfaces," Phys. Rev. Lett. **93**, 257805 (2004).
[47]E. Brunet and A. Ajdari, "Generalized Onsager relations for electrokinetic effects in anisotropic and heterogeneous geometries," Phys. Rev. E **69**, 016306 (2004).

Downloaded 13 Aug 2013 to 131.216.164.149. This article is copyrighted as indicated in the abstract. Reuse of AIP content is subject to the terms at: http://pof.aip.org/about/rights_and_permissions